

Influence of road salt thawing peaks on the inflow composition and activated sludge properties in municipal wastewater treatment

J. Tauber , B. Flesch, V. Parravicini , K. Svardal  and J. Krampe 

ABSTRACT

Operational data over 2 years from three large Austrian wastewater treatment plants (WWTPs) with design capacities of 4 million, 950,000 and 110,000 population equivalent (PE) were examined. Salt peaks, due to thawing road salt were detected and quantified by electrical conductivity, temperature and chloride measurement in the inflow of the WWTPs. Daily NaCl inflow loads up to 1,147 t/d and PE-specific loads of 0.26–0.5 kg NaCl/(PE · y) were found. To mimic the plants' behaviour in a controlled environment, NaCl was dosed into the inflow of a laboratory-scale activated sludge plant. The influence of salt peaks on important activated sludge parameters such as sludge volume index, settling velocity and floc size were investigated. Influent and effluent were sampled extensively to calculate removal rates. Respiration measurements were performed to quantify activated sludge activity. Particle size distributions of the activated sludge floc sizes were measured using laser diffraction particle sizing and showed a decrease of the floc size by approximately two-thirds. The floc structure was examined and documented using light microscopy. At salt concentrations below 1 g/L, increased respiration was found for autotrophic biomass, and between 1 and 3 g NaCl/L respiration was inhibited by up to 30%.

Key words | activated sludge, NaCl shock loading, oxygen uptake rate, particle size, sludge volume index

HIGHLIGHTS

- Yearly, 7–12 thawing road-salt events of up to 3 g NaCl/L were detected at WWTPs.
- Approx. 25% of the salt applied yearly in public areas was found in the WWTPs' inflow.
- Respiration increased for concentrations <1 g NaCl/L and decreased above them.
- Autotrophic activity OUR_A (+42%) was enhanced by more than heterotrophic OUR_H (+20%).
- Sludge floc particle size decreased by two-thirds after salt shocks.

INTRODUCTION





Activated sludge parameters, like sludge volume index (SVI) and settling velocity (v_s), are crucial for the design of activated sludge plants. The total suspended solids (TSS) concentration

in the effluent of the secondary clarifier and thus the retention of mixed liquor suspended solids (MLSS) in the aeration tank are important performance indicators (DWA 2016). The oxygen uptake rate (OUR) of the activated sludge gives important information about the process performance and the plant's capacity (Cech *et al.* 1985; Hagman & Jansen 2007).

In the winter, road salt, mainly NaCl, is spread on the streets. Hoffman *et al.* (2011) reported that in Austria

This is an Open Access article distributed under the terms of the Creative Commons Attribution Licence (CC BY 4.0), which permits copying, adaptation and redistribution, provided the original work is properly cited (<http://creativecommons.org/licenses/by/4.0/>).

doi: 10.2166/wst.2021.045

J. Tauber  (corresponding author)
 B. Flesch
 V. Parravicini 
 K. Svardal 
 J. Krampe 
 Institute for Water Quality and Resource
 Management,
 TU Wien, Karlsplatz 13/226, 1040 Vienna,
 Austria
 E-mail: jtauber@iwag.tuwien.ac.at

117,000–377,000 t/y (271,000 t/y on average) salt is used for street de-icing, with NaCl being most common salt, while <10% other salts, mostly CaCl₂, are used. With precipitation and snowmelt, high loads of road salt are flushed into the sewer systems (combined sewers) and transported to the wastewater treatment plants (WWTPs). At knowledge-exchange events for operators, Austrian WWTP operators have reported negatively affected effluent quality caused by bulking sludge after road-salt events, but there has been no proven evidence for the correlation.

The influence of highly saline wastewater on the activity of activated sludge has been studied by different authors worldwide. [Aslan & Simsek \(2012\)](#) described the inhibitory effects on nitrite oxidizing bacteria (NOB) due to NaCl peaks and that ammonium oxidizing bacteria (AOBp) activity was more affected than NOB activity. [Wang *et al.* \(2005\)](#) performed inhibition tests with NaCl concentrations up to 20 g/L and reported reduced oxygen uptake rate and total organic carbon (TOC) removal for salinity peaks with concentrations greater than 0.5 g NaCl/L. [Salvadó *et al.* \(2001\)](#) reported a reduction of the protozoa biomass in activated sludge at NaCl concentrations between 3 and 10 g NaCl/L and a total abundance of protozoa between 20 and 40 g/L. [Perneti & Di Palma \(2005\)](#) reported that after a few weeks of adaption (depending on the operating conditions) activated sludge was able to adapt to 30–50 g NaCl/L. In this adaption phase, the settling properties of the activated sludge were reduced and the volatile suspended solids (VSS) specific oxygen uptake rate (sOUR) was inhibited by up to 80%. It should be noted that this study was performed using synthetic wastewater. Most of the studies in the literature report that activated sludge is able to adapt on highly saline conditions after several weeks ([Panswad & Anan 1999](#); [Wang *et al.* 2005](#); [Bassin *et al.* 2011](#); [Aslan & Simsek 2012](#)).

All these studies found in the literature were performed using batch tests or very high salt concentrations (up to 40 g NaCl/L), which are representative for industrial wastewater or seawater-influenced WWTPs, but not transferable to municipal and non-seawater-influenced WWTPs affected by short thawing road-salt events in wintertime. Activated sludge in industrial and seawater-influenced WWTPs is adapted to high chloride and salt concentrations. It is hypothesized that in municipal WWTPs where the activated sludge is not adapted to high salt concentrations, salt shocks caused by thawing road salt during the wintertime can affect the plants' operational and treatment efficiency. In particular, changes in settling and flocculation behaviour due to thawing road salt peaks can affect the plants' operational performance. When temperatures are low, salt-related inhibition effects also can affect the WWTPs' performance because the sludge

age is higher than the salt's influence, there is not enough time for the biomass to adapt to increased salt concentrations.

This study focuses on the impact of short-term road-salt events on municipal WWTPs caused by road de-icing in wintertime. To gain information about typical NaCl salt concentrations and loads, three WWTPs with different catchment area structures, sewer systems and design capacities were investigated. Dosing experiments were performed in a continuous working laboratory-scale plant with a total volume of 375 L to investigate the salt's impact on not unadapted activated sludge.

MATERIAL AND METHODS

Operational data from three Austrian WWTPs were evaluated: WWTP A with a 4 million population equivalent (PE), WWTP B with a 950,000 PE and WWTP C with a 110,000 PE design capacity based on COD₁₂₀ (120 g chemical oxygen demand (COD) per PE and day). All three plants are designed for biological nutrient removal based on the activated sludge process and additional chemical phosphorus precipitation. Daily hydraulic inflow, electrical conductivity (EC) and temperature were used to model NaCl concentrations and loads in the plants' inflow. For this, a polynomial model according to [Lewis & Perkin \(1978\)](#) was applied. At WWTP B and C additional chloride concentration measurements in the inflow were taken according to DIN EN ISO 10304-1. With this data, chemical stoichiometry also allows the calculation of daily NaCl inflow concentrations and loads.

WWTP A's catchment area is mostly urban with a relatively small industrial impact and a combined sewer system. [Figure 1\(a\)](#) shows EC and temperature data of the inflow of WWTP A. The wintertime (November 1st–April 30th) is marked with boxes. [Figure 1\(b\)](#) shows the cumulative distribution function of the EC in the inflow. Thawing road-salt events at WWTP A caused by road de-icing in the wintertime were detected through high EC values (>1,800 µS/cm) in the plant's inflow and cross-checked with precipitation data. 15 thawing road-salt events were identified in wintertime within 2 years, and these are highlighted with a box ([Figure 1\(b\)](#)).

WWTP B is strongly influenced by industrial wastewater. Approximately 8.5% of the hydraulic inflow and 25% of the organic load (as chemical oxygen demand; COD) is the result of industrial discharge. WWTP B has a large catchment with a mixture of urban and rural areas, and the sewage is mainly collected through a combined sewer system (>90% of the inflow). [Figure 2\(a\)](#) shows the hydraulic inflow and temperature in the inflow of WWTP B. Due to the industrial impact,

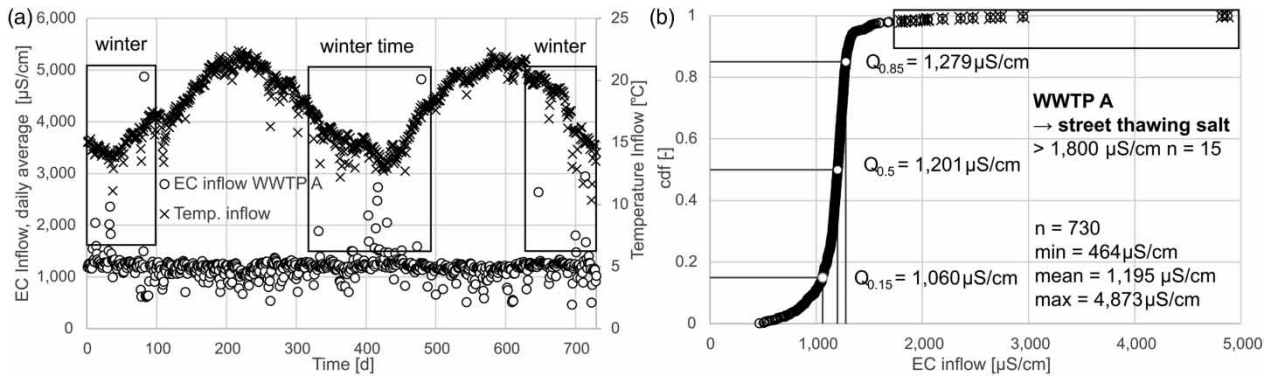


Figure 1 | (a) Electrical conductivity (EC) and temperature data in the inflow of WWTP A over 2 years. (b) Cumulative distribution function (cdf) of EC in the inflow of WWTP A.

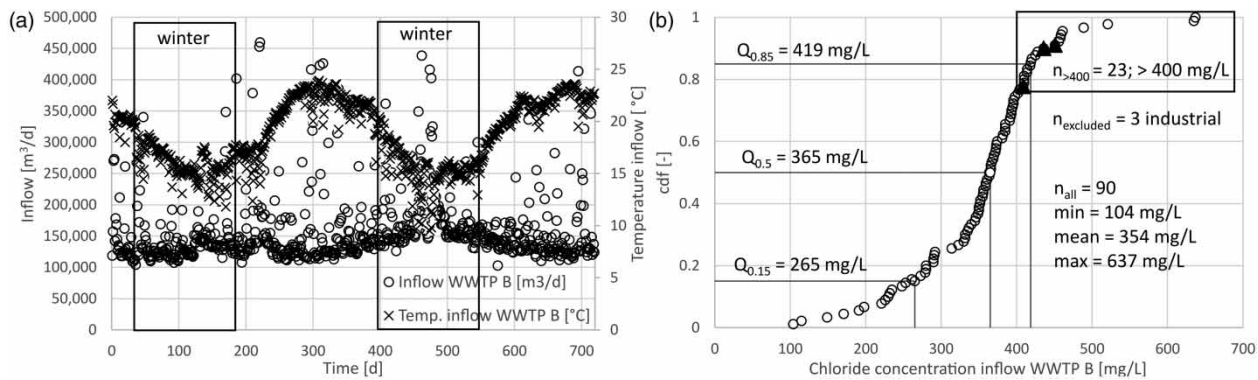


Figure 2 | (a) inflow and temperature in the inflow of WWTP B. (b) Cumulative distribution function (cdf) of the chloride inflow concentration at WWTP B; 23 values >400 mg/L are marked with a box of which three excluded values are marked with triangles.

the inflow temperature in the winter is mostly above 15 °C. The chloride concentrations in the inflow are also strongly influenced by the industrial discharge (mean = 354 mg/L). Thawing road-salt events were detected at WWTP B through high chloride concentrations (>400 mg Cl⁻/L) in the plant's inflow and cross-checked with precipitation data. 23 events with high chloride concentrations were detected. Three values with concentrations >400 mg/L were caused by

industrial discharge and are not connected to thawing road salt. These three events are marked with triangles in Figure 2(b) and were excluded from the load calculations.

WWTP C is located in a rural area with a low industrial impact. The sewer system is partly combined and partly separate. Daily chloride measurements were carried out at this plant. Figure 3(a) shows daily chloride loads in the inflow of WWTP C over 3 years. Figure 3(b) shows the cumulative

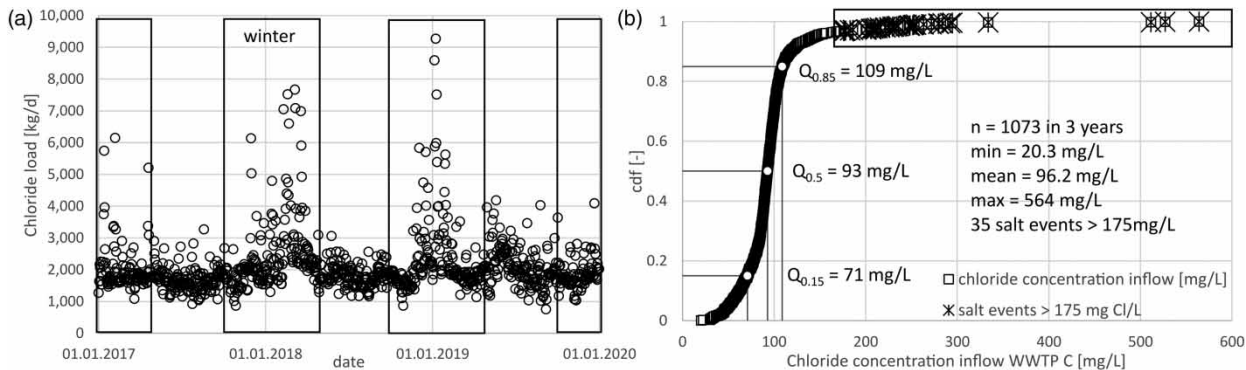


Figure 3 | (a) Chloride loads in the inflow of WWTP C. (b) Cumulative distribution function (cdf) of the daily chloride inflow concentration at WWTP C.

distribution function of the chloride concentration in the inflow of WWTP C. The mean chloride concentration in the inflow is 96.2 mg Cl⁻/L. Thawing road-salt events at WWTP C were detected through high chloride concentrations (>175 mg Cl⁻/L) in the plant's inflow and cross-checked with precipitation data.

Thawing road salt concentration and load

The inflow NaCl concentration (c_{NaCl}) for WWTP A was calculated using a polynomic model with temperature and conductivity data as inputs (Equations (1)–(4)). This conductivity method (Lewis & Perkin 1978) is most commonly used to calculate salinity. S is the salinity concentration, ΔS is the coefficient of temperature dependence, R_t is a function of concentration and temperature, t denotes the temperature and C the conductivity, coefficients a_0 to a_5 and b_0 to b_5 are empiric factors (Table 1).

$$S = a_0 + a_1 R_t^{\frac{1}{2}} + a_2 R_t + a_3 R_t^{\frac{3}{2}} + a_4 R_t^2 + a_5 R_t^{\frac{5}{2}} + \Delta S \quad [\text{g/L}] \quad (1)$$

$$\Delta S = \left[\frac{t - 15}{1 + 0.0162(t - 15)} \right] \times (b_0 + b_1 R_t^{\frac{1}{2}} + b_2 R_t + b_3 R_t^{\frac{3}{2}} + b_4 R_t^2 + b_5 R_t^{\frac{5}{2}}) \quad [\text{g/L}] \quad (2)$$

$$C_{\text{NaCl}} = -0.0267243 * t^3 + 4.6636947 * t^2 + 861.302764 * t + 29,035.1640651 \quad [\mu\text{S/cm}] \quad (3)$$

$$R_t = \frac{C_{\text{Sample},t}}{C_{\text{NaCl},t}} \quad [-] \quad (4)$$

At WWTP B and WWTP C daily NaCl loads were calculated using the Cl⁻ load.

Laboratory-scale experiments

Laboratory experiments were performed using a continuous flow single-stage activated sludge plant with pre-denitrification and a volume of 375 L. The laboratory-scale plant was operated with an aerobic sludge age of approximately 13.5 days, to achieve biological nutrient (N and P) removal without additional chemical phosphorus precipitation. To mimic

the behaviour of thawing road-salt events in full-scale plants, salt was dosed in the inflow continuously for 24 hours to reach a concentration of 3 g NaCl/L in the aeration tank for 24 hours. The salt-dosing experiment was repeated five times with a break of 1–3 weeks between them. The activated sludge was examined before, during and after the salt dosing using different methods. To calculate removal rates, inflow and effluent were sampled twice a week for COD, NH₄-N, NO_x-N, NO₂-N, total nitrogen (TN), PO₄-P, total phosphorus (TP), suspended solids (SS) and volatile solids (VS) concentrations. A list of the methods used can be found in Table S1, Supplementary Information. The sludge volume (SV) was measured to calculate the sludge volume index (SVI) according to Dick & Vesilind (1969). The settling velocity (v_s) was measured using a 1 L graduated cylinder and the floc size was investigated as described below. The wastewater used for the laboratory-scale experiments was extracted from the sewer network of the campus of TU Wien and contained 766 mg/L COD, 41 mg/L NH₄-N, 3.8 mg/L PO₄-P, 63 mg/L TN and 6.1 mg/L TP ($n = 29$) in average.

Light microscopy and particle size distribution

Before, during and after the salt dosing tests, images were taken using light microscopy to evaluate the activated sludge floc size and structure as well as changes in the protozoa community. The sludge floc size was measured using laser diffraction particle sizing (Malvern Mastersizer 2000). Particle size distributions were calculated as the mean of five single measurements of every sludge sample with a minimum of 20,000 particles (activated sludge flocs) each.

Respiration measurements

Respiration measurements were performed to evaluate the oxygen uptake rates of the activated sludge. Autotrophic (OUR_A), heterotrophic (OUR_H), as well as maximum autotrophic (OUR_{Amax}) and maximum heterotrophic (OUR_{Hmax}) were measured in WWTP B (i.e. at full scale) and at laboratory scale while the salt-dosing tests were performed. The detailed procedure is described in Nowak & Svoldal (1993).

Table 1 | Empiric coefficients a and b for the conductivity method according to Lewis & Perkin (1978)

a_0 0.008	a_1 -0.1692	a_2 -25.3851	a_3 -14.0941	a_4 -7.0261	a_5 2.7081
b_0 0.0005	b_1 -0.0056	b_2 -0.0066	b_3 -0.0375	b_4 0.0636	b_5 -0.014

RESULTS AND DISCUSSION

Impact on the inflow composition (concentration and load)

A cross check of the NaCl loads was performed for WWTP A. Figure 4(a) shows exemplary calculated daily inflow concentrations and salinity loads originating from thawing road-salt events at WWTP A. Up to 3 g NaCl/L was detected in the inflow of the WWTP. Figure 4(b) shows thawing road-salt events and their calculated corresponding NaCl loads. In 2 years, 15 road-salt events with loads between 5 and 1,147 t/d were detected. The average load was 267 t NaCl/d. Summing up all 15 events leads to a yearly NaCl load in the inflow of approximately 2,000 t NaCl/y.

Compared to the 12,000 t NaCl/y used for de-icing in the catchment area (MA 48 2018; Wien Holding 2019) and considering that surfaces with no sewer connection, such as highways are also salted in the winter, the calculated salt load fits well with the quantities of salt applied. Salt aerosol deposition by swirling up also has to be considered, and it is in the range of up to 15% in urban areas (GSF 2005).

At WWTP B the calculation of NaCl inflow loads is affected by the high chloride background concentrations

caused by a strong industrial impact. At WWTP B, 23 salt events with loads between 3.7 and 91.6 t/d were detected in 2 years. The average load was 26.2 t NaCl/d. Summing up all 23 events leads to a yearly NaCl load in the inflow of 249 t NaCl/y. At WWTP C 35 salt events with loads between 0.15 and 14.9 t/d were detected in 2 years. The average load per event was 4 t NaCl/d. The yearly NaCl load as a result of de-icing activities in the inflow of WWTP C was 46 t NaCl/y. The cumulative distribution function of the NaCl inflow loads at WWTP B and WWTP C caused by thawing road-salt events can be found in the Supplementary Information. Cumulative distribution functions of NaCl inflow loads caused by thawing road-salt events can be found in the Supplementary Information (Figure S1).

As expected, the calculated NaCl inflow loads for the three observed Austrian WWTPs showed a link between size and structure of the catchment area and the salt loads in the inflow. In mostly urban areas with a combined sewer system, a high proportion of the thawing road-salt applied for street de-icing ends up in the WWTP.

Table 2 gives an overview of the WWTPs' design capacity, their catchment area, the average number of yearly thawing road-salt events, the yearly additional salt load in the inflow and the additional PE-specific yearly

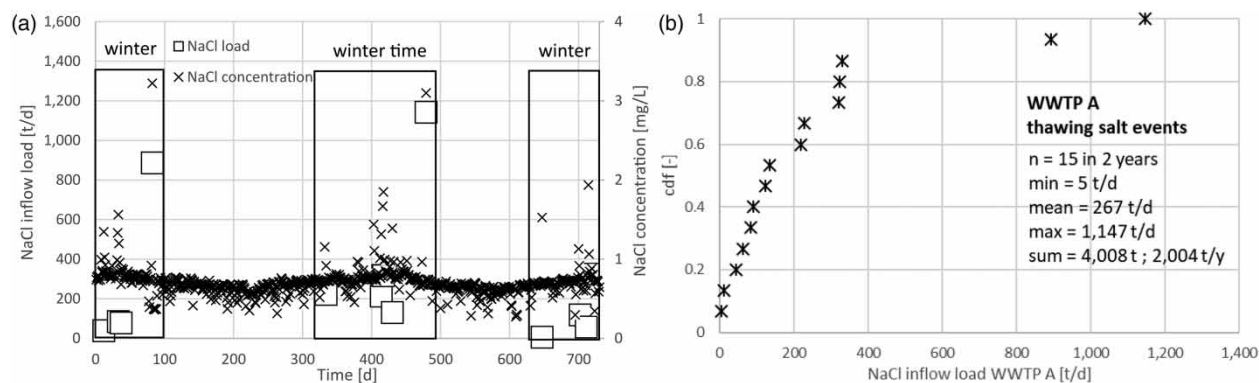


Figure 4 | (a) Daily NaCl inflow concentrations and loads from thawing road-salt events are marked with boxes. (b) Cumulative distribution function (cdf) of the daily inflow loads to WWTP A due to thawing road-salt events in 2 years.

Table 2 | Comparison of the catchment area, design capacity, yearly thawing road-salt loads and PE-specific road salt loads for the three WWTPs considered

WWTP	Catchment area Structure	Design Capacity PE _{cod}	Yearly road-salt events 1/y	Yearly road-salt load t NaCl/y	PE-specific road-salt load from winter maintenance kg NaCl/(PE · y)
A	Urban	4 million	7.5	2,004	0.50
B	Urban/rural	950,000	10	249	0.26
C	Rural	110,000	12	46	0.42

salt load from winter maintenance. It should be noted, that other salt loads, for example of industrial origin, are not included.

On average, 7.5–12 thawing road-salt events per year were detected. It should be noted that WWTP A and WWTP C are located in the eastern part of the country, where winters are not as cold and snowy as in the western part, where WWTP B is located.

The PE-specific additional salt load caused by thawing road salt ranges between 0.26 and 0.5 kg NaCl/(PE · y). The highest value can be explained by the highly urban structure of the catchment area of WWTP A, while WWTP B is more rural, where more of the sewer system is separate. In this area deadening grit is used on the streets. Even though in the catchment area of WWTP C road salt and deadening grit are used, the highest number of road-salt events (12 y^{-1}) leads to a relatively high additional PE-specific road-salt load related to winter maintenance.

Impact of thawing salt on sludge properties and plant operation

Using usual operational data, no effect of thawing road salt on the parameters SS, VS and SVI was found at the full-scale plants, because of seasonal and random fluctuations. To exclude these fluctuations, five dosing experiments were performed at laboratory scale. Each experiment lasted for 5 days, with a pause of 1–2 weeks between the salt dosages. Figure 5 gives an overview of the SVI, SS and VS values during three dosing experiments (I–III).

Average SVI increased from 107 ml/g in the reference timeframe (April–June 2019) to 147 ml/g on average (maximum 346 ml/g) when salt was dosed three times (June–August 2019). The SS concentration in the aeration tank decreased from 6 to 4.9 g/L while the aerobic sludge age was held at 13.5 days. The settling velocity decreased from

1.7 to 0.5 m/h on average. This had an effect on the effluent quality, caused by slight sludge drift of small flocs. All full- and laboratory-scale SS values were 3.5–7 g/L.

Light microscopy and particle size distribution

Microscopic examination of the activated sludge showed that the average floc size (d_p) decreased from approximately 1,000 μm (Figure 6(a)) before salt dosing to approximately 200 μm (Figure 6(b)) 5 days after salt dosing.

Laser diffraction particle sizing also showed a decrease of the sludge floc size. In Figure 7(a) comparison of the measured particle size distributions of the laboratory-scale plant's activated sludge before and 5 days after the salt dosing can be found.

The 10th percentile, mean and 90th percentile values of the volume-equivalent spherical diameter of the sludge flocs show that the size decreased. The average sludge floc size was 209.5 μm before dosing and 69.4 μm 5 days after it. The 10th percentile and 90th percentile of the floc size fell from 79.9 to 17.3 μm and from 470.8 to 204 μm respectively. Considering that measured particle sizes are volume-equivalent spherical diameters and activated sludge flocs are mostly not spherical, this explains the difference between the size measured using the light microscope and values from laser diffraction particle sizing. Both methods showed a decrease in the floc size of approximately two-thirds because of flocs falling apart due to road-salt events. These particle size data correlated well with the changes in SVI, as shown above. As was observed in the dosing experiments I–III, the flocs falling apart caused a decrease in the SS concentration in the aeration tank and an associated increase in the SVI. At the same time the SS concentration in the secondary settling tank effluent increased from approximately 10 mg/L to 15–20 mg/L, but the average daily excess sludge removal rate was not

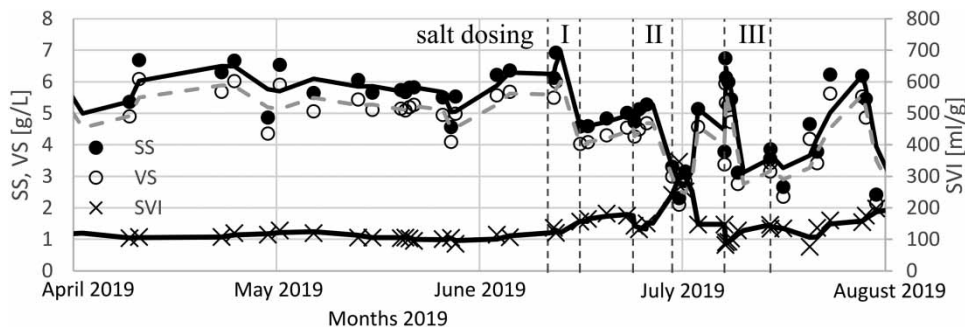


Figure 5 | SS, VS and SVI for the reference timeframe (April–June 2019) and three salt dosing experiments (I–III) (June–August 2019). The lines for SS (solid line) and VS (dashed line) indicate a moving average over two values.

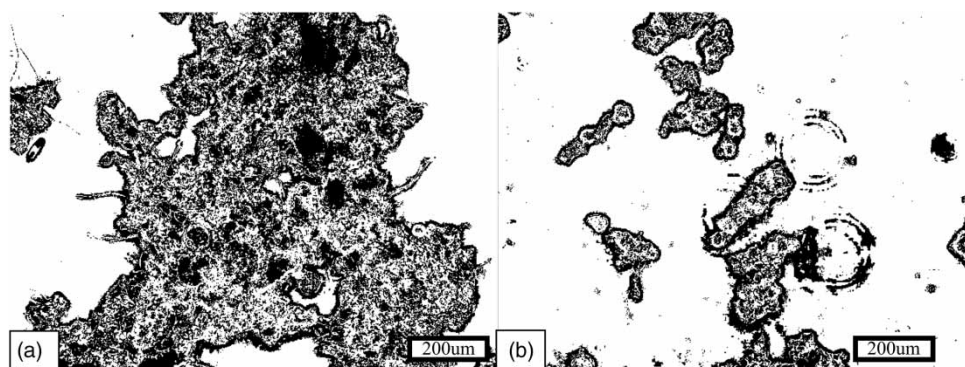


Figure 6 | Phase contrast images of activated sludge flocs (a) before and (b) 5 days after 3 g NaCl/L dosage for 24 hours.

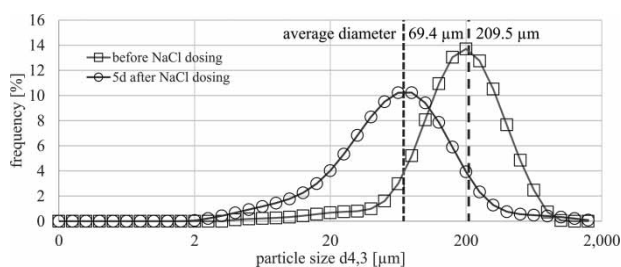


Figure 7 | Particle size distributions of the activated sludge flocs before and 5 days after salt dosing; $d_{4,3}$ denotes the volume-equivalent spherical diameter.

reduced for this period to exclude other effects on the treatment plant during the salt dosing tests.

Simultaneous to the flocs falling apart, unusually high extracellular polymeric substances (EPS) production was detected. pH and oxygen probes in the laboratory-scale aeration tank were covered with a thick layer of bacterial slime, which led to measured oxygen concentrations being wrong, with an absolute error of up to 4 mg O₂/L only 5 hours after cleaning the probes.

Table 3 summarizes removal rates and effluent concentrations of COD, TN, NH₄-N and PO₄-P of the laboratory-scale plant before, during and after salt dosing. The inflow concentration for COD was 699 mg/L and 64.3 mg/L on average for TN, while NH₄-N and PO₄-P inflow concentrations were on average 42.2 mg/L and 4.1 mg/L, respectively.

The COD and TN removal rates were on average 94% and 81% before the salt dosing. During the salt dosing they were 98% and 84%, changing to 96% and 86% 5 days after the salt dosing. During the salt dosing the NH₄-N and PO₄-P effluent concentrations were the lowest, on average, during the experiments but within 1.22 mg/L and 0.76 mg/L, respectively, of the normal fluctuation range. It should be noted that no chemical phosphorus precipitation was performed.

Respiration measurements

Autotrophic and heterotrophic oxygen uptake rates and effluent quality (TSS, N and P) were affected by salt peaks. Respiration tests showed an increase of OUR_H and OUR_A 3 hours after the beginning of salt dosing and a decrease to normal levels after 80 hours. This pattern was found in the laboratory-scale and the full-scale data (WWTP B).

Figure 8 shows a comparison of organic dry matter (ODM)-specific oxygen uptake rate (sOUR) values between full-scale (8a) and laboratory-scale data (8b) for salt events with a concentration of 0.7 g NaCl/L. OUR_{Cg} denotes the endogenous carbon respiration, OUR_{Cs} the substrate respiration (substrate is dosed to match the plant's organic load), OUR_{Cmax} the maximum carbon respiration, OUR_{NH4} the maximum NH₄ respiration, OUR_{NO2} the maximum NO₂

Table 3 | Removal rates and effluent concentrations of the laboratory-scale plant before, during and after salt dosing

Sampling time	Number of samples	Removal rates		Number of samples	Effluent concentration	
		COD %	TN %		NH ₄ -N mg/L	PO ₄ -P mg/L
Before salt dosing	$n = 33$	94	81	$n = 32$	1.76	1.16
During salt dosing	$n = 7$	98	84	$n = 9$	1.22	0.76
5 days after salt dosing	$n = 5$	96	86	$n = 6$	2.26	1.40

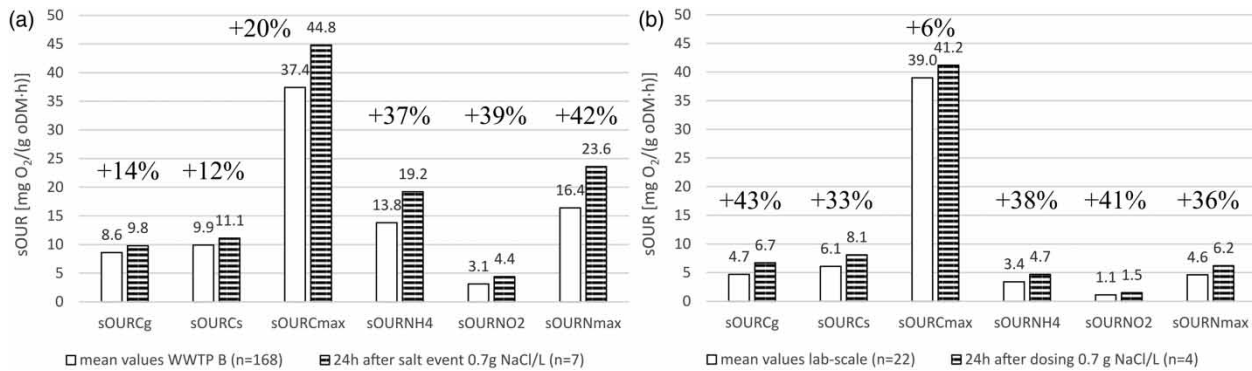


Figure 8 | Comparison between specific oxygen uptake rates at full scale (WWTP B) (a) and laboratory scale (b).

respiration and $OUR_{N_{max}}$ the maximum nitrogen ($NH_4 + NO_2$) respiration.

Data from 168 respiration measurements at WWTP B were evaluated. Respiration measurements approximately 24 hours after road-salt events at WWTP B (seven events) showed an increase of the ODM-specific oxygen uptake rates. At WWTP B sOURs increased between +12% for $sOUR_{C_s}$ and +42% for $sOUR_{A_{max}}$.

Data from 22 respiration measurements at laboratory scale were evaluated. 24 hours after salt dosing all values increased (6–43%). Measurements at laboratory scale showed similar results, with an increase in the sOUR between 6% for $sOUR_{C_{max}}$ and approximately 40% for $sOUR_{NH_4}$, $sOUR_{NO_2}$ and $sOUR_{N_{max}}$. At both full and laboratory scales OUR_A (OUR_{NH_4} , OUR_{NO_2} and $OUR_{N_{max}}$), with $sOUR_{N_{max}}$ increasing by 42%, was more affected than OUR_H (OUR_{C_g} , OUR_{C_s} and $OUR_{C_{max}}$), with $sOUR_{C_{max}}$ increasing by 20%. With similar inflow conditions and elevated salt concentrations in the inflow, the bacterial activity at laboratory scale showed the same behaviour as at full scale. It is suspected that this elevated activity is related to bacterial protection mechanisms, such as additional EPS production. Above a critical concentration of approximately 1 g NaCl/L, the inhibiting effects are suspected to be caused by osmotic effects superimposed on the positive increase in activity.

CONCLUSION AND SUMMARY

Different methods were applied to calculate inflow salt concentrations and loads for three large WWTPs. Depending on the catchment area, PE-specific yearly salt loads of between 0.26 and 0.5 kg NaCl/(PE · y) from thawing road-salt events in winter were found.

Salt dosing tests were performed at laboratory scale to mimic the full-scale inflow conditions. These results

showed a decrease in the average floc size of approximately two-thirds and sludge flocs falling apart after dosing the plant's inflow with salt.

The activated sludge's oxygen uptake rates were influenced by the inflow's salt concentration. Respiration measurements showed an increased respiration at concentrations below 1 g NaCl/L and decreased respiration at concentrations between 1 g NaCl/L and 3 g NaCl/L. At both full and laboratory scales, autotrophic respiration was more affected than heterotrophic respiration.

Despite the high amounts of road salt in the full- and laboratory-scale plants' inflows operational and analytic parameters showed that the effluent quality was not negatively affected, apart from a slight increase in the SS concentration in the effluent of the secondary settling tank at the laboratory-scale plant which remained within the limit values of 20 mg/L suspended solids. This indicates a sufficiently high sludge age to guarantee full nitrification and denitrification ability, even if salt-related inhibitions occur. But if the plant's capacity is already fully used, this has to be considered in future, especially for autotrophic conversion rates.

The unexpectedly high EPS production found at laboratory scale, led to a severe impairment of the oxygen concentration measurement and the aeration control. This can be attributed to a bacterial protective mechanism. At the three full-scale WWTPs investigated, no such salt-triggered EPS production was found, so it is suspected that the biomass at full scale was already adapted to low salt concentrations caused by smaller road-salt events during wintertime.

Overall, laboratory tests showed that thawing road-salt events had an influence on biological wastewater treatment. At low salt concentrations, a positive effect was shown by increased respiration, probably caused by a change in the osmotic pressure on the bacterial cell walls, which makes

them more permeable. At higher concentrations, there were negative effects on respiration. However, the negative effects were less than expected and in the three full-scale systems the level of inhibition was not the same as in the laboratory test.

DATA AVAILABILITY STATEMENT

All relevant data are included in the paper or its Supplementary Information.

REFERENCES

- Aslan, S. & Simsek, E. 2012 Influence of salinity on partial nitrification in a submerged biofilter. *Bioresource Technology* **118**, 24–29. doi:10.1016/j.biortech.2012.05.057.
- Bassin, J. P., Pronk, M., Muyzer, G., Kleerebezem, R., Dezotti, M. & van Loosdrecht, M. C. M. 2011 Effect of elevated salt concentrations on the aerobic granular sludge process: linking microbial activity with microbial community structure. *Applied and Environmental Microbiology* **77** (22), 7942–7953. doi:10.1128/AEM.05016-11.
- Cech, J. S., Chudoba, J. & Grau, P. 1985 Determination of kinetic constants of activated sludge microorganisms. *Water Science and Technology* **17** (2–3), 259–272. doi:10.2166/wst.1985.0135.
- Dick, R. I. & Vesilind, P. A. 1969 The sludge volume index: what is it? *Journal Water Pollution Control Federation* **41**, 1285–1291. doi: 10.1016/0043-1354(82)90056-2.
- DWA 2016 STANDARD A 131E. *Dimensioning of Single-Stage Activated Sludge Plants*. Theodor-Heuss-Allee 17, 53773 Hennef, Germany: DWA Deutsche Vereinigung für Wasserwirtschaft, Abwasser und Abfall e.V./German Association for Water, Wastewater and Waste.
- GSF-Forschungszentrum für Gesundheit und Umwelt in der Helmholtz Gemeinschaft 2005 *Hintergrundinformation: Feinstaubquelle Streusalz? – Pro und Contra im Einsatz gegen Schnee und Glatteis. (Background Information: Fine Dust Source of Road Salt? Pros and Cons in Action Against Snow and Black Ice)*. Available from: <https://www.helmholtz-muenchen.de/fileadmin/GSF/pdf/presse/2005/Streusalz.pdf> (accessed 10 October 2020).
- Hagman, M. & Jansen, J. L. C. 2007 *Oxygen Uptake Rate Measurements for Application at Wastewater Treatment Plants*. Vatten, pp. 131–138. Available from: https://www.tidskriftenvatten.se/wp-content/uploads/2017/04/48_article_2361.pdf (accessed 10 October 2020).
- Hoffman, M., Blab, R. & Nutz, P. 2011 *Optimierung der Feuchtsalzstreuung (Optimization of Wet Salt Spreading) Final Report, Federal Ministry Republic of Austria Climate Action, Environment, Energy, Mobility, Innovation and Technology*. p. 118. Available from: https://www.bmk.gv.at/themen/verkehr/strasse/verkehrssicherheit/vsf/forschungsarbeiten/15_feuchtsalzstreuung.html (accessed 11 January 2021).
- Lewis, E. L. & Perkin, R. G. 1978 Salinity: its definition and calculation. *Journal of Geophysical Research* **83**, 203–206. doi: 10.1029/JC083iC01p00466.
- MA 48 2018 *Streudiens, Wien die versalzene Stadt (Street Thawing Service, Vienna the Salty City) Press Release*. Available from: <https://www.derstandard.at/story/2000076715904/wien-die-versalzene-stadt> (accessed 5 June 2020).
- Nowak, O. & Svardal, K. 1993 Observations on the kinetics of nitrification under inhibiting conditions caused by industrial wastewater compounds. *Water Science and Technology* **28** (2), 15–123. <https://doi.org/10.2166/wst.1993.0088>.
- Panswad, T. & Anan, C. 1999 Specific oxygen, ammonia, and nitrate uptake rates of a biological nutrient removal process treating elevated salinity wastewater. *Bioresource Technology* **70** (3), 237–243. doi: 10.1016/S0960-8524(99)00041-3.
- Pernetti, M. & Palma, L. D. 2005 Experimental evaluation of inhibition effects of saline wastewater on activated sludge. *Environmental Technology* **26** (6), 695–704. doi: 10.1080/09593330.2001.9619509.
- Salvadó, H., Mas, M., Menéndez, S. & Gracia, P. 2001 Effects of shock loads of salt on protozoan communities of activated sludge. *Acta Protozool* **40**, 177–185.
- Wang, J. L., Zhan, X. M., Feng, Y. C. & Qian, Y. 2005 Effect of salinity variations on the performance of activated sludge system. *Biomedical and Environmental Sciences* **18**, 5–8.
- Wien Holding 2019 *Streusalz (Street Thawing Salt)*. Available from: <https://www.stadt-wien.at/wien/news/streusalz.html> (accessed 7 June 2020).

First received 15 November 2020; accepted in revised form 22 January 2021. Available online 4 February 2021